

Seismic analysis of series isolation system based on geometry nonlinearity

Z D Lin, H Shi, L Xue

City Institute, Dalian Univ. of Tech., Dalian, China

Abstract. According to the system of rubber bearing serially connected with column, the mathematical model of serially isolated system based on geometric nonlinear is investigated by using Hamilton's principle. The effects of axial pressure and difference column size to the series isolation system in seismic response is discussed. The series isolation system dynamics model based on geometric nonlinear is established considering the cross section rotated and the influence of the shear deformation and axial pressure. The differential quadrature element method is employed for discrete processing on governing equations and boundary conditions. Seismic response of series isolation system subjected to the far-field ground motions is solved numerically. Results show that: the slenderness ratio of cantilever column will significantly affect the seismic response of the isolation system under far-field ground motions, and it is particularly to response of the cantilever column.

1. Introduction

In recent seismic isolation projects, a new design method of seismic isolation that installs laminated rubber bearing onto top of the column in basement is highlighted and gradually attracts the attention of the project field. The design guarantees the sufficient use of internal and lower space and saves costs. In 1999, based on researches by Gent^[4] and Kelly^[5-6], Zhou^[1, 2] et al. and Zhou^[3] constructed the static model of capital serially connected seismic isolation system and deduced the horizontal stiffness equation and critical load equation of capital serially connected seismic isolation system. Regarding capital seismic isolation structure, Ma^[9] et al. proposed the iterative-free computation corresponding to P- Δ effect motivation and analyzed the influence of P- Δ effect on capital seismic isolation structure. Qi^[10-11] et al. discussed the design method of first-floor structure capital seismic isolation technique and tested dynamic characteristics of a five-floor framework structure that applies first-floor structure capital seismic isolation technique under environment inspiration and initial displacement condition. Pan^[12] et al. reinforced the six-floor framework structure whose ground floor is weaker in Du Jiangyan City that was involved in Wenchuan Earthquake with application of setting lead laminated rubber bearing to first-floor capital and analyzed the dynamic characteristics and earthquake reaction of the structure after reinforcement. As results indicate, reinforced structure can satisfy the requirement of improving fortifying and effectively improve the seismic isolation function of the structure. Thus, in order to further explore dynamic characteristics of serially connected seismic isolation system, in addition to overall analysis on dynamic response of serially connected seismic isolation structure, detailed analysis should be conducted on the seismic isolation system of laminated rubber bearing and column serially connected.

On the basis of homogeneous laminated rubber bearing theory, the dynamic response control equation of serially connected seismic isolation system based on geometric nonlinearity is deduced; with application of differential quadrature element method (DQEM) ^[13-15], the equation and boundary conditions are dispersed; finally, the earthquake response to the system is solved numerically.



Corresponding observation object is obtained and the influence of axial force and slenderness ratio of suspended column on seismic isolation functions of serially connected seismic isolation system is discussed by using numerical results. These results provide foundation for further researches on the dynamic behaviours of serially connected seismic isolation structure.

2. Analysis Model of Serially Connected Seismic Isolation System

As shown in Figure 1 and Figure 2, considering that the total height of serially connected seismic isolation system is H with laminated rubber seismic isolation bearing on the top, the laminated structure consisting of steel plates and rubber sheets is simplified as equivalent, continuous and uniform columns. Meanwhile, considering the influence of bend deformation and shear deformation, the cross section is A_r ; the diameter is d ; equivalent density is ρ_r ; modified bend elastic modulus is E_r ; shear modulus is G_r ; moment of inertia of cross section is I_r . The lower part is reinforced concrete column, to which the seismic isolation bearing is connected at the height of h . The cross section is A_c ; equivalent density is ρ_c ; elastic modulus is E_c ; shear modulus is G_c and moment of inertia of cross section is I_c . The other side $y = 0$ is connected to the foundation.

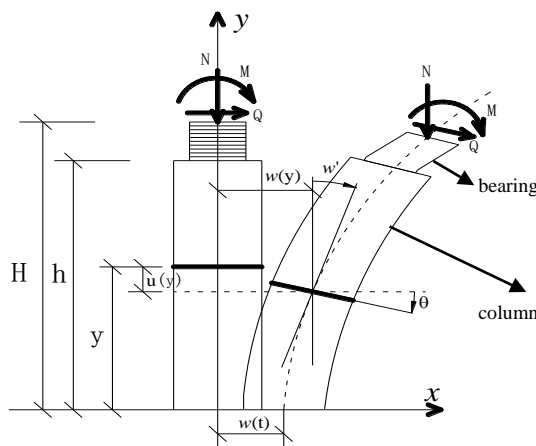


Figure 1. Deformation pattern for serially connected isolation

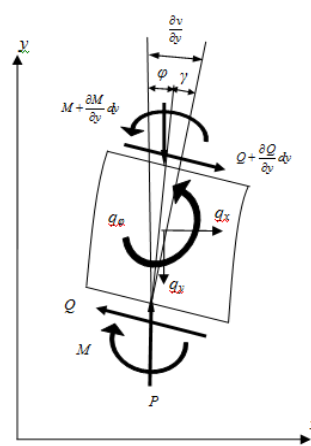


Figure 2. Differential element

3. Control Equation and Boundary Conditions

The center line of homogeneous column is y -axis and the symmetry axis of cross section is x -axis, according to first-class shear deformation beam theory, the displacement fields are listed as below:

$$\begin{cases} U_y = u(y,t) - x\varphi(y,t) \\ U_x = v(y,t) \end{cases} \quad (1)$$

In the equation, u and v refer to the vertical and horizontal displacement on the column center line, respectively; φ refers to the normal angle of cross section after deformation.

Based on the displacement fields mentioned above, under the framework of limited deformation, the nonlinear geometric equation can be obtained as below:

$$\begin{cases} \epsilon_y = \frac{\partial u}{\partial y} + \frac{1}{2} \left(\frac{\partial v}{\partial y} \right)^2 - x \frac{\partial \varphi}{\partial y} \\ \gamma_{yx} = \frac{\partial v}{\partial y} - \varphi \end{cases} \quad (2)$$

It can be seen from the beam theory that as for homogeneous column, if linear and isotropic elastic materials are assumed, the constitutive equation is:

$$\sigma_y = E \varepsilon_y, \tau_{yx} = G \gamma_{yx}, G = \frac{E}{2(1 + \mu)} \quad (3)$$

In the equation, E refers to the modified bend elastic modulus of laminated rubber bearing; G refers to shear modulus; μ refers to Poisson ratio.

In order to deduce the motion differential equation, boundary conditions and initial condition that displacement, u , v and φ , of geometric nonlinear elastic homogeneous column structure satisfy, Hamilton variation principle is applied. In satisfying geometric nonlinear equation, displacement and boundary conditions and enabling all the possible displacement of designated motion at the initial and termination moment, the actual displacement, u , v and φ , make the functional select stationary values.

$$\Pi = \int_0^T H dt = \int_0^T -(U - W - T) dt \quad (4)$$

In the equation, $H = -(U - W - T)$ refers to Hamilton function and T refers to kinetic energy of the structure; $U = U_1 + U_2$ refers to strain energy and U_1 and U_2 refer to the strain energy raised by normal strain and shear strain respectively; W refers to the work applied by horizontal external load and axial force.

With introduction of the concept of finite element, serially connected seismic isolation system can be divided into two units and \bar{e} that is marked in the variable's upper right means the unit No. e. $\bar{e} = \bar{1}$ refers to the steel concrete column unit in the lower part and $\bar{e} = \bar{2}$ refers to the laminated rubber seismic isolation bearing unit in the upper part. $v^{\bar{1}}(y, t)$, $u^{\bar{1}}(y, t)$ and $\theta^{\bar{1}}(y, t)$ are recorded as the cross section angles that is initiated by horizontal displacement, vertical displacement and bending of steel concrete column in the lower part, respectively; meanwhile, $v^{\bar{2}}(y, t)$, $u^{\bar{2}}(y, t)$ and $\theta^{\bar{2}}(y, t)$ refer to the cross section angles that is initiated by horizontal displacement, vertical displacement and bending of laminated rubber bearing in the upper part; thus, the motion control equation of geometric nonlinear serially connected seismic isolation system is:

$$\left\{ \begin{array}{ll} \rho^{\bar{1}} A^{\bar{1}} \ddot{u}^{\bar{1}} - E^{\bar{1}} A^{\bar{1}} \frac{\partial^2 u^{\bar{1}}}{\partial y^2} - E^{\bar{1}} A^{\bar{1}} \frac{\partial v^{\bar{1}}}{\partial y} \frac{\partial^2 v^{\bar{1}}}{\partial y^2} - p = 0 & 0 < y < h \\ \rho^{\bar{1}} A^{\bar{1}} \frac{\partial^2 v^{\bar{1}}}{\partial t^2} + P \frac{\partial^2 v^{\bar{1}}}{\partial y^2} - E^{\bar{1}} A^{\bar{1}} \frac{\partial^2 u^{\bar{1}}}{\partial y^2} \frac{\partial v^{\bar{1}}}{\partial y} - E^{\bar{1}} A^{\bar{1}} \frac{\partial u^{\bar{1}}}{\partial y} \frac{\partial^2 v^{\bar{1}}}{\partial y^2} - \frac{3}{2} E^{\bar{1}} A^{\bar{1}} \left(\frac{\partial v^{\bar{1}}}{\partial y} \right)^2 \frac{\partial^2 v^{\bar{1}}}{\partial y^2} \\ - \kappa^{\bar{1}} G^{\bar{1}} A^{\bar{1}} \left(\frac{\partial^2 v^{\bar{1}}}{\partial y^2} - \frac{\partial \varphi^{\bar{1}}}{\partial y} \right) - q = 0 & 0 < y < h \\ \rho^{\bar{1}} I^{\bar{1}} \frac{\partial^2 \varphi^{\bar{1}}}{\partial t^2} - E^{\bar{1}} I^{\bar{1}} \frac{\partial^2 \varphi^{\bar{1}}}{\partial y^2} - \kappa^{\bar{1}} G^{\bar{1}} A^{\bar{1}} \left(\frac{\partial v^{\bar{1}}}{\partial y} - \varphi^{\bar{1}} \right) = 0 & 0 < y < h \\ \rho^{\bar{2}} A^{\bar{2}} \ddot{u}^{\bar{2}} - E^{\bar{2}} A^{\bar{2}} \frac{\partial^2 u^{\bar{2}}}{\partial y^2} - E^{\bar{2}} A^{\bar{2}} \frac{\partial v^{\bar{2}}}{\partial y} \frac{\partial^2 v^{\bar{2}}}{\partial y^2} - p = 0 & h < y < H \\ \rho^{\bar{2}} A^{\bar{2}} \frac{\partial^2 v^{\bar{2}}}{\partial t^2} + P \frac{\partial^2 v^{\bar{2}}}{\partial y^2} - E^{\bar{2}} A^{\bar{2}} \frac{\partial^2 u^{\bar{2}}}{\partial y^2} \frac{\partial v^{\bar{2}}}{\partial y} - E^{\bar{2}} A^{\bar{2}} \frac{\partial u^{\bar{2}}}{\partial y} \frac{\partial^2 v^{\bar{2}}}{\partial y^2} - \frac{3}{2} E^{\bar{2}} A^{\bar{2}} \left(\frac{\partial v^{\bar{2}}}{\partial y} \right)^2 \frac{\partial^2 v^{\bar{2}}}{\partial y^2} \\ - \kappa^{\bar{2}} G^{\bar{2}} A^{\bar{2}} \left(\frac{\partial^2 v^{\bar{2}}}{\partial y^2} - \frac{\partial \varphi^{\bar{2}}}{\partial y} \right) - q = 0 & h < y < H \\ \rho^{\bar{2}} I^{\bar{2}} \frac{\partial^2 \varphi^{\bar{2}}}{\partial t^2} - E^{\bar{2}} I^{\bar{2}} \frac{\partial^2 \varphi^{\bar{2}}}{\partial y^2} - \kappa^{\bar{2}} G^{\bar{2}} A^{\bar{2}} \left(\frac{\partial v^{\bar{2}}}{\partial y} - \varphi^{\bar{2}} \right) = 0 & h < y < H \end{array} \right. \quad (5)$$

Coordination conditions:

There are internal boundary conditions (coordination conditions) including displacement coordination conditions and internal force balance conditions between steel concrete column and laminated rubber bearing:

$$\begin{cases} u^{\bar{1}} = u^{\bar{2}}, v^{\bar{1}} = v^{\bar{2}}, \varphi^{\bar{1}} = \varphi^{\bar{2}} & y = h \\ M^{\bar{1}} = M^{\bar{2}}, Q^{\bar{1}} = Q^{\bar{2}}, N^{\bar{1}} = N^{\bar{2}} & y = h \end{cases} \quad (6)$$

Boundary conditions are:

$$\begin{cases} u = 0, v = 0, \varphi = 0, \frac{\partial v}{\partial y} = 0 & y = 0 \\ E_r A_r \left[\frac{\partial u}{\partial y} + \frac{1}{2} \left(\frac{\partial v}{\partial y} \right)^2 \right] = m_t \frac{\partial^2 u}{\partial t^2} + m_t \left(\frac{\partial \varphi}{\partial t} \right)^2 - p & y = H \\ \kappa_r G_r A_r \left(\frac{\partial v}{\partial y} - \varphi \right) - m_t g \frac{\partial v}{\partial y} = -m_t g \frac{\partial^2 v}{\partial t^2} - m_t e \frac{\partial^2 \varphi}{\partial t^2} + q & y = H \\ E_r I_r \frac{\partial \varphi}{\partial y} = -(J_t + m_t e^2) \frac{\partial^2 \varphi}{\partial t^2} - m_t e \frac{\partial^2 v}{\partial t^2} + e q & y = H \\ \varphi = 0, \frac{\partial v}{\partial y} = 0 & y = H \end{cases} \quad (7)$$

Initial conditions:

If homogeneous column remains in natural status when $t < 0$, the following initial conditions can be satisfied when $t \geq 0$:

$$\begin{aligned} u|_{t=0} &= 0, \dot{u}|_{t=0} = 0; \\ v|_{t=0} &= 0, \dot{v}|_{t=0} = 0; \\ \varphi|_{t=0} &= 0, \dot{\varphi}|_{t=0} = 0; \end{aligned} \quad (8)$$

4. Different Quadrature Method

In essence, different quadrature method uses the weighted sum of node function values in the whole universe to express the approximate values of partial derivative of function at a certain point and adopts high Lagrange polynomial in the whole universe to approximate a certain continuous function to be solved in the universe. As for the serially connected seismic isolation system that is researched in this paper, different quadrature method is utilized in the two units including laminated rubber bearing and suspended column. In other words, n nodes are selected in the direction of y and according to the different quadrature principle^[16-19], equation (5) is dispersed in the interval of $[0, 1]$. The different quadrature form is:

$$\left\{ \begin{aligned}
 & \rho^{\bar{e}} A^{\bar{e}} \ddot{u}_{i0}^{\bar{e}}(A_{10}, A_{20}) + \rho^{\bar{e}} A^{\bar{e}} \ddot{u}_{i0}^{\bar{e}}(A_{10}, A_{20}) \begin{bmatrix} A_{11} & A_{21} \\ A_{12} & A_{22} \end{bmatrix} + \rho^{\bar{e}} A^{\bar{e}} (\ddot{u}_{i1}^{\bar{e}}, \ddot{u}_{i2}^{\bar{e}}) \begin{bmatrix} A_{11} & A_{21} \\ A_{12} & A_{22} \end{bmatrix}^2 \\
 & - \Delta t^2 \frac{E^{\bar{e}} A^{\bar{e}}}{H^2} \left(\sum_{j=1}^n B_{ij} \ddot{u}_{j1}^{\bar{e}}, \sum_{j=1}^n B_{ij} \ddot{u}_{j2}^{\bar{e}} \right) - \Delta t^2 \frac{E^{\bar{e}} A^{\bar{e}}}{H^3} \left(\sum_{j=1}^n A_{ij} v_{j1}^{\bar{e}} \sum_{j=1}^n B_{ij} v_{j2}^{\bar{e}}, \sum_{j=1}^n A_{ij} v_{j2}^{\bar{e}} \sum_{j=1}^n B_{ij} v_{j1}^{\bar{e}} \right) \frac{\partial^2 u^{\bar{e}}}{\partial y^2} - \Delta t^2 \rho^{\bar{e}} A^{\bar{e}} (\ddot{u}_{g1}, \ddot{u}_{g2}) = 0 \\
 & \rho^{\bar{e}} A^{\bar{e}} \dot{v}_{i0}^{\bar{e}}(A_{10}, A_{20}) + \rho^{\bar{e}} A^{\bar{e}} \dot{v}_{i0}^{\bar{e}}(A_{10}, A_{20}) \begin{bmatrix} A_{11} & A_{21} \\ A_{12} & A_{22} \end{bmatrix} + \rho^{\bar{e}} A^{\bar{e}} (v_{i1}^{\bar{e}}, v_{i2}^{\bar{e}}) \begin{bmatrix} A_{11} & A_{21} \\ A_{12} & A_{22} \end{bmatrix}^2 \\
 & + \Delta t^2 \frac{P}{H^2} \left(\sum_{j=1}^n B_{ij} v_{j1}^{\bar{e}}, \sum_{j=1}^n B_{ij} v_{j2}^{\bar{e}} \right) - \Delta t^2 \frac{E^{\bar{e}} A^{\bar{e}}}{H^3} \left(\sum_{j=1}^n B_{ij} u_{j1}^{\bar{e}} \sum_{j=1}^n A_{ij} v_{j1}^{\bar{e}}, \sum_{j=1}^n B_{ij} u_{j2}^{\bar{e}} \sum_{j=1}^n A_{ij} v_{j2}^{\bar{e}} \right) \frac{\partial^2 u^{\bar{e}}}{\partial y^2} \\
 & - \Delta t^2 \frac{E^{\bar{e}} A^{\bar{e}}}{H^3} \left(\sum_{j=1}^n A_{ij} u_{j1}^{\bar{e}} \sum_{j=1}^n A_{ij} v_{j1}^{\bar{e}}, \sum_{j=1}^n B_{ij} u_{j2}^{\bar{e}} \sum_{j=1}^n A_{ij} v_{j2}^{\bar{e}} \right) - \frac{3}{2} \Delta t^2 \frac{E^{\bar{e}} A^{\bar{e}}}{H^4} \left[\left(\sum_{j=1}^n A_{ij} v_{j1}^{\bar{e}} \right)^2 \sum_{j=1}^n B_{ij} v_{j1}^{\bar{e}}, \left(\sum_{j=1}^n A_{ij} v_{j2}^{\bar{e}} \right)^2 \sum_{j=1}^n B_{ij} v_{j2}^{\bar{e}} \right] \\
 & - \Delta t^2 G^{\bar{e}} A^{\bar{e}} \left[\frac{1}{H^2} \sum_{j=1}^n B_{ij} v_{j1}^{\bar{e}} - \frac{1}{H} \sum_{j=1}^n A_{ij} \phi_{j1}^{\bar{e}}, \frac{1}{H^2} \sum_{j=1}^n B_{ij} v_{j2}^{\bar{e}} - \frac{1}{H} \sum_{j=1}^n A_{ij} \phi_{j2}^{\bar{e}} \right] - \Delta t^2 \rho^{\bar{e}} A^{\bar{e}} (\ddot{v}_{g1}, \ddot{v}_{g2}) = 0 \\
 & \rho^{\bar{e}} I^{\bar{e}} \dot{\phi}_{i0}^{\bar{e}}(A_{10}, A_{20}) + \rho^{\bar{e}} I^{\bar{e}} \dot{\phi}_{i0}^{\bar{e}}(A_{10}, A_{20}) \begin{bmatrix} A_{11} & A_{21} \\ A_{12} & A_{22} \end{bmatrix} + \rho^{\bar{e}} I^{\bar{e}} (\phi_{i1}^{\bar{e}}, \phi_{i2}^{\bar{e}}) \begin{bmatrix} A_{11} & A_{21} \\ A_{12} & A_{22} \end{bmatrix}^2 \\
 & - \Delta t^2 \frac{E^{\bar{e}} I^{\bar{e}}}{H^2} \left(\sum_{j=1}^n B_{ij} \phi_{j1}^{\bar{e}}, \sum_{j=1}^n B_{ij} \phi_{j2}^{\bar{e}} \right) - \Delta t^2 G^{\bar{e}} A^{\bar{e}} \left(\frac{1}{H} \sum_{j=1}^n A_{ij} v_{j1}^{\bar{e}} - \phi_{j1}^{\bar{e}}, \frac{1}{H} \sum_{j=1}^n A_{ij} v_{j2}^{\bar{e}} - \phi_{j2}^{\bar{e}} \right) - \Delta t^2 \rho^{\bar{e}} A^{\bar{e}} (\ddot{u}_{g1}, \ddot{u}_{g2}) = 0
 \end{aligned} \right. \tag{9}$$

In the equation above, A_{ij} and B_{ij} refer to weighting coefficients that are determined by the following equations, respectively:

$$C_{ij}^{(1)} = \begin{cases} \frac{\prod_{\substack{l=1 \\ l \neq i, l \neq j}}^n (x_i - x_l)}{\prod_{\substack{l=1 \\ l \neq j}}^n (x_j - x_l)}, & (i, j = 1, 2, \dots, n, j \neq i) \\ \sum_{\substack{l=1 \\ l \neq i}}^n \frac{1}{x_i - x_l}, & (i, j = 1, 2, \dots, n, j = i) \end{cases} \tag{10}$$

When $r=2, 3, \dots, n-1$,

$$C_{ij}^{(r)} = \begin{cases} r \left(A_{ii}^{(r-1)} A_{ij}^{(1)} - \frac{A_{ij}^{(r-1)}}{x_i - x_j} \right), & (i, j = 1, 2, \dots, n, j \neq i) \\ - \sum_{\substack{l=1 \\ l \neq i}}^n A_{il}^{(r)}, & (i = 1, 2, \dots, n) \end{cases} \tag{11}$$

The different quadrature form of boundary conditions is:

$$\left\{ \begin{array}{l}
 u^{\bar{1}} = 0, v^{\bar{1}} = 0, \varphi^{\bar{1}} = 0; \\
 \frac{E^{\bar{2}} A^{\bar{2}}}{H^2} \left[\sum_{j=1}^n A_{nj} u_{j1}^{\bar{2}} + \frac{1}{2H} \left(\sum_{j=1}^n A_{nj} v_{j1}^{\bar{2}} \right)^2, \sum_{j=1}^n A_{nj} u_{j1}^{\bar{2}} + \frac{1}{2H} \left(\sum_{j=1}^n A_{nj} v_{j1}^{\bar{2}} \right)^2 \right] - P = 0 \\
 \Delta t^2 G^{\bar{2}} A^{\bar{2}} \left(\frac{1}{H} \sum_{j=1}^n A_{nj} v_{j1}^{\bar{2}} - \varphi_{j1}^{\bar{2}}, \frac{1}{H} \sum_{j=1}^n A_{nj} v_{j2}^{\bar{2}} - \varphi_{j2}^{\bar{2}} \right) - \Delta t^2 PH \left(\sum_{j=1}^n A_{nj} v_{j1}^{\bar{2}}, \sum_{j=1}^n A_{nj} v_{j2}^{\bar{2}} \right) \\
 + m_i v_{n0}^{\bar{2}} (A_{10}, A_{20}) + m_i v_{n0}^{\bar{2}} (A_{10}, A_{20}) \begin{bmatrix} A_{11} & A_{21} \\ A_{12} & A_{22} \end{bmatrix} + m_i v_{n0}^{\bar{2}} (v_{n1}^{\bar{2}}, v_{n2}^{\bar{2}}) \begin{bmatrix} A_{11} & A_{21} \\ A_{12} & A_{22} \end{bmatrix}^2 - \Delta t^2 m_i (\ddot{v}_{g1}, \ddot{v}_{g2}) = 0 \\
 \Delta t^2 \frac{E^{\bar{2}} I^{\bar{2}}}{H} \left(\sum_{j=1}^n A_{nj} \varphi_{j1}^{\bar{2}}, \sum_{j=1}^n A_{nj} \varphi_{j2}^{\bar{2}} \right) + m_i e v_{n0}^{\bar{2}} (A_{10}, A_{20}) + m_i e v_{n0}^{\bar{2}} (A_{10}, A_{20}) \begin{bmatrix} A_{11} & A_{21} \\ A_{12} & A_{22} \end{bmatrix} \\
 + m_i e v_{n0}^{\bar{2}} (v_{n1}^{\bar{2}}, v_{n2}^{\bar{2}}) \begin{bmatrix} A_{11} & A_{21} \\ A_{12} & A_{22} \end{bmatrix}^2 - \Delta t^2 m_i e (\ddot{v}_{g1}, \ddot{v}_{g2}) = 0 \\
 \varphi^{\bar{2}} = 0;
 \end{array} \right. \quad (12)$$

The Chebyshev-Gauss-Lobatto grid points in normalized interval [0,1] will be employed in this work.

$$x_i = \frac{1}{2} \left[1 - \cos \left(\frac{i-1}{n-1} \pi \right) \right], (i = 1, 2, \dots) \quad (13)$$

Substitution method is used to handle with boundary conditions. With combination of equation (9) and (12), dynamic response solution is conducted.

5. Numerical Analysis and Discussion

5.1. Analysis on seismic wave used

In order to analyze the response principle of serially connected seismic isolation system under the effect of far-field earthquake, the far-field (the distance from epicentre is larger than 10km) earthquake record that is recommended by ATC-63 is applied, as shown in Table 1.

Table 1. Recommended far-field earthquakes sets by ATC-63

No.	Magnitude	Year	Name	Seismic station	Component
1	6.7	1994	Northridge	Beverly Hills-Mulhol	NGA_no_953_MUL279
2	6.7	1994	Northridge	Canyon Country-WLC	NGA_no_960_LOS270
3	7.1	1999	Duzce,Turkey	Bolu	NGA_no_1602_BOL090
4	7.1	1999	Hector Mine	Hector	NGA_no_1787_HEC090
5	6.5	1979	Imperial Valley	Delta	NGA_no_169_H-DLT352
6	6.5	1979	Imperial Valley	EI Centro Array # 11	NGA_no_174_H-E11230
7	6.9	1995	Kobe,Japan	Nishi-Akashi	NGA_no_1111_NIS090
8	6.9	1995	Kobe,Japan	Shin-Osaka	NGA_no_1116_SHI090
9	7.5	1999	Kocaeli,Turkey	Duzce	NGA_no_1158_DZC270
10	7.5	1999	Kocaeli,Turkey	Arcelik	NGA_no_1148_ARC090
11	7.3	1992	Landers	Yermo Fire Station	NGA_no_900_YER360
12	7.3	1992	Landers	Coolwater	LANDERS_CLW_TR
13	6.9	1989	Loma Prieta	Capitola	NGA_no_752_CAP090
14	6.9	1989	Loma Prieta	Gilroy Array #3	NGA_no_767_GO3090

15	7.4	1990	Manjil,Iran	Abhar	MANJIL_ABBAR_T
16	6.5	1987	Superstition	EI Centro Imp.Co	NGA_no_721_B-ICC090
17	6.5	1987	Superstition	Poe Road(temp)	NGA_no_725_B-POE360
18	7.0	1992	Cape Mendocino	Rio Dell Overpass	NGA_no_829_RIO360
19	7.6	1999	Chi-Chi,Taiwan	CHY101	NGA no 1244 CHY101-N
20	7.6	1999	Chi-Chi,Taiwan	TCU045	CHICHI_TCU045_N
21	6.6	1971	San Fernando	LA-Hollywood Stor	NGA_no_68_PEL180
22	6.5	1976	Friuli,Italy	Tolmezzo	NGA_no_125_A-TMZ270

5.2 parameter selection of serially connected seismic isolation system

As examined, in actual projects, the density degree of concrete is C30; elastic modulus $E=3.0e10$ Pa; shear shape factor $K=0.845$. LRB500 product parameters of a company in Nanjing are selected for seismic isolation bearing (see Table 2); the shear shape factor of seismic isolation bearing $K=0.899$.

Table 2. Parameters of rubber bearings (LRB500)

Diameter (mm)	Lead's Diameter (mm)	Rubber underlayer thickness (mm)	Rubber underlayer number	Total thickness of rubber underlayer (mm)	Steel thickness (mm)	Steel number	Top steel thickness (mm)
500	100	4.8	20	96	2	19	15
G (GPa)	Height (mm)	s1	s2	Vertical stiffness (kN/mm ²)	50% eq. horizontal stiffness (kN/m)	250% eq. horizontal stiffness (kN/m)	250% eq. damping ratio
0.392	164	26	5.2	1634	2257	956.1	0.169

According to article 6.4.1, 6.4.2, 11.4.11 and 11.4.16 in Design Code of Concrete Structure (version 2010), 6.2.15 in Technical Specification of Concrete Structure of High-rise Buildings (version 2010) and 3.4.2 in Guide for Design and Construction of Basic Seismic Isolation Structure, with comprehensive consideration of seismic grade, axial-compression ratio of reinforced concrete framework, stability coefficient of reinforced concrete components and size of pre-embedded steel plates, the size of suspended column is selected as shown in Table 3.

Table 3. Geometric size of reinforced concrete column

Column height (m)	Sectional dimension of square column (m)									
3.0	0.4	0.5	0.6	0.65	0.7	0.75	0.8	0.9	1.0	1.0
3.6	0.45	0.5	0.6	0.7	0.8	0.95	1.0	1.1	1.2	1.2
4.2	0.5	0.6	0.7	0.8	0.9	1.0	1.1	1.2	1.3	1.3
4.8	0.6	0.7	0.8	0.9	1.0	1.1	1.25	1.4	1.5	1.5

5.3 result analysis

With application of MATLAB language, programs are edited and node number in each section is 11. In numerical calculation, the peak value of earthquake wave is adjusted to a rare level of 0.2g for each grade, that is, 400cm/s^2 .

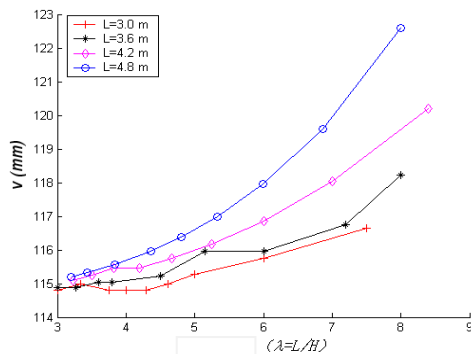


Figure 3. Average displacement curves of rubber bearing at top point

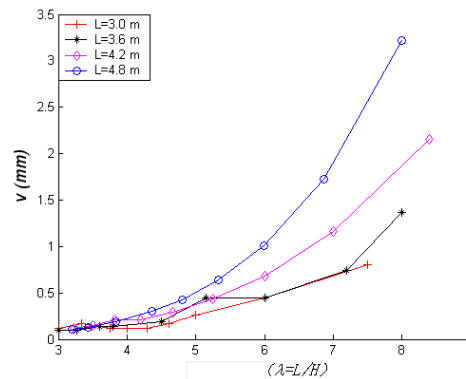


Figure 4. Average displacement curves of column at top point

It can be seen from Figure 3 that the top displacement of serially connected seismic isolation system bearing apparently increases as the slenderness ratio increases. Slope change rate of each curve has proved it. When the slenderness ratio is determined, the higher the column is, the gentler the system appears. Thus, the peak value of displacement is larger. Only under the effect of axial load of 10MPa, the maximum value of rare earthquake top displacement response of LRB500 laminated rubber bearing is close to 300mm, which will greatly decrease the safety of serially connected seismic isolation system.

The dynamic stability of serially connected seismic isolation system depends on seismic isolation bearing and suspended column. Figure 4 shows the average values of top displacement of suspended column corresponding to different slenderness ratio. The figures aim at comparatively analyzing the influence of different slenderness ratio on top displacement of independent column. As shown in the figure, under the effect of far-field ground motions, influences of the slenderness ratio of independent column on the top of shock insulation cushion and the top of detached column are entirely different.

6. Conclusion

According to the research results that laminated rubber bearing is supposed to be homogeneous column, the dynamical control equations of series seismic isolation system based on geometric nonlinearity are deduced by Hamilton variation principle; kinematic equation and boundary conditions of rubber bearing unit and cantilever column unit are established based on finite element method; numerical solution is conducted by using different quadrature element method, the relatively mature mathematical method. At 10MPa vertical load, the dynamic response of series seismic isolation system of slenderness ratio of different cantilever column under effect of far-field ground motions are calculated respectively. The numerical results show that under effect of far-field ground motions, with increase of slenderness ratio of cantilever column, stiffness degradation of series seismic isolation system decreases, lateral displacement of the top of cantilever column increases, and dynamic response of the top of shock insulation cushion is gently changing. On this basis, change of axial load leads to significant increase of dynamic response of series seismic isolation system, which seriously influences the stability of series seismic isolation system and finally results in decrease of integral security of isolated structure.

References

- [1] Zhou X Y , Han M , Zeng D M and Ma D H 1999 Horizontal Rigidity Coefficient of the Serial System of Rubber Bearing with Column *J. of Vibration Engineering* **12(2)** 157-165

- [2] Zhou X Y , Han M , Zeng D M 1999 Calculation method of lateral stiffness of combined rubber bearing and serial system of bearing with columns *J. of EARTHQUAKE ENGINEERING AND ENGINEERING VIBRATION* **19(4)** 67-75
- [3] Zhou J 2000 Horizontal Rigidity Coefficient of the Serial System of Rubber Bearing with Column *J. of Engineering Mechanics* **3(3)** 45-49
- [4] Gent A N 1964 Elastic stability of rubber compression springs *J. Engineering Mechanics* **6(4)** 318–326
- [5] Koh C G, Kelly J M A 1988 Simple mechanical model for electrometric bearings used in base isolation *Journal of Engineering Mechanics* **30(12)** 933–943
- [6] Ryan K L, Kelly J M and Chopra A K 2005 Nonlinear Model for Lead-Rubber Bearings Including Axial-load Effects *Journal of Engineering Mechanics* **131(12)** 1270-1278
- [7] Kelly J M 2003 Tension buckling in multilayer elastomeric bearings *Journal of Engineering Mechanics* **129(12)** 1363-1368
- [8] Kelly J M 1997 *Earthquake resistant design with rubber* (London: Spriger)
- [9] Ma C F, Tan P, Zhang Y H, Zhou F L 2010 Dynamic responses analysis of structures with isolators on the top of the columns considering $P - \Delta$ effects. *CHINA CIVIL ENGINEERING JOURNAL* **43** 230-234
- [10] Wu Y X, Qi A 2011 Application of Isolation Technology on the Top of Columns for First-floor Weak Frame-structure, *J. of Yanbian Univ.(Natural Science)* **33(4)** 349-354
- [11] Wu Y X, Qi A 2011 Study on test of dynamic properties for a first-floor isolation structure *J. of EARTHQUAKE ENGINEERING AND ENGINEERING VIBRATION* **31(6)** 147-152
- [12] Pan P, Cao H Y, Qi Y J 2009 Retrofit of Soft First Story Structure Using Seismic Isolation Technology *J. of Earthquake Resistant Engineering and Retrofitting* **31(6)** 69-73
- [13] Wang X W, Bert C W 1993 A new approach in applying differential quadrature to static and free vibration analyses of beams and plates *J. Sound and Vibration* **162(3)** 566-572
- [14] Wang X W, Liu F, Wang X F and Gan L F 2005 New approaches in application of differential quadrature method to fourth-order differential equations *Commun. Numer. Meth. Engng* **21** 61-71
- [15] Liu G R, Wu T Y 2001 VIBRATION ANALYSIS OF BEAMS USING THE GENERALIZED DIFFERENTIAL QUADRATURE RULE AND DOMAIN DECOMPOSITION *Journal of Sound and Vibration* **246(3)** 461-481
- [16] Du Y Y, Lin Z D, Li H 2012 Dynamic characteristics of a system of rubber bearings serially connected with columns *J. of VIBRATION AND SHOCK* **31(17)** 134-139.
- [17] Li J J, Hu Y J, Cheng C J and Zheng J 2010 Differential quadrature method for nonlinear dynamical behavior of a viscoelastic Timoshenko beam *J. of VIBRATION AND SHOCK* **29(4)** 143-145.
- [19] Fung T C 2001 Solving initial value problems by differential quadrature method- Part II : second-and higher-order equations *International Journal for Numerical Methods in Engineering* **50** 1429-1457